
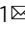


Switchable bifunctional molecular recognition in water using a pH-responsive *Endo*-functionalized cavity

Xiaoping Wang¹, Mao Quan¹, Huan Yao¹, Xin-Yu Pang¹, Hua Ke¹ & Wei Jiang¹  

The construction of water-soluble synthetic hosts with a stimuli-responsive *endo*-functionalized cavity is challenging. These hosts feature a switchable cavity and may bring new properties to the fields of self-assembly, molecular machines, and biomedical sciences. Herein, we report a pair of water-soluble naphthotubes with a pH-responsive *endo*-functionalized cavity. The inward-directing secondary amine group of the hosts can be protonated and deprotonated. Thus, the hosts have different cavity features at the two states and show drastically different binding preference and selectivity in water. We reveal that the binding difference of the two host states is originated from the differences in charge repulsion, hydrogen bonding and the hydrophobic effects. Moreover, the guest binding can be easily switched in a ternary mixture with two guest molecules by adjusting the pH value of the solution. These pH-responsive hosts may be used for the construction of smart self-assembly systems and water-soluble molecular machines.

¹Shenzhen Grubbs Institute, Guangdong Provincial Key Laboratory of Catalysis, and Department of Chemistry, Southern University of Science and Technology, Xueyuan Blvd 1088, 518055 Shenzhen, China. ✉email: jiangw@sustech.edu.cn

Selective molecular recognition in water is the basis of numerous biological processes¹, such as enzyme catalysis, biological assemblies, transmembrane transportation, signal transduction, and biological machines. Synthetic receptors with the ability of selective molecular recognition in water may provide new tools for chemical biology, environmental sciences, analytical chemistry and biomedical sciences. However, it is difficult for synthetic hosts to achieve selective molecular recognition in water^{2–13}. It would require effective use of hydrogen bonding in water, which is however very challenging^{14,15}. During the last decades, several biomimetic hosts^{16–24} have been developed and they are able to selectively recognize organic molecules in water through shielded hydrogen bonding and the hydrophobic effects. These synthetic hosts show potential in noncovalent bioconjugation²⁵, chiroptical sensing^{26,27}, adsorption removal of polar organic pollutants from water²⁸, and spectroscopic detection of biomarkers^{29,30}.

Nevertheless, the binding properties of these hosts are not stimuli-responsive. Introducing stimuli-responsiveness would bring new properties in molecular recognition and self-assembly^{31–38}. If stimuli-responsive groups are merged into the inward-pointing groups of these hosts, it would provide new tools for switchable noncovalent bioconjugation³⁹, drug delivery systems⁴⁰, water-soluble molecular machines^{41–46}, and easily recovered host-based adsorption materials^{47–49}. To address this, it requires a water-soluble synthetic host with a stimuli-responsive *endo*-functionalized cavity.

Over the past years, we have reported a series of macrocyclic hosts with an *endo*-functionalized cavity^{24,50}. Of them, water-soluble amide naphthotubes (**1a** and **1b**, Fig. 1a) were shown to be able to selectively recognize a wide scope of organic molecules^{51–57} in water by effectively employing shielded hydrogen bonding and the hydrophobic effects. In addition, protonated amine naphthotubes (**2a**•6H⁺ and **2b**•6H⁺, Fig. 1b) are able to bind organic carboxylates in water through buried salt

bridges and the hydrophobic effects⁵⁸. Amine naphthotubes **2a** and **2b** have the potential to be pH-responsive^{59,60}, but have to exist in acidic condition to maintain water solubility. Nevertheless, on this basis, new naphthotubes may be designed to realize a stimuli-responsive *endo*-functionalized cavity.

Herein, we report a pair of naphthotubes with a pH-responsive *endo*-functionalized cavity which are able to perform switchable bifunctional molecular recognition in water. One amide group and one secondary amine group are incorporated into the naphthotubes as the inward-directing functional groups. In addition, four carboxylate groups are installed as the sidechains to provide water solubility at the pH range in which protonation and deprotonation of the secondary amine group are allowed. Thus, this pair of naphthotubes possesses a pH-responsive *endo*-functionalized cavity. In the protonated and deprotonated states, the cavity features of the naphthotubes are totally different and thus they show different binding preference and selectivity to guests. The guest binding can be simply switched by adjusting the pH value of the solution.

Results and discussion

Design, synthesis and characterization. Initially, we thought the pH-responsive naphthotubes should be easy to construct. Amine naphthotubes **2a** and **2b** provide a good basis. In order to maintain the water solubility and to achieve pH responsiveness simultaneously, the water-soluble groups on amine naphthotubes **2a** and **2b** were changed from the primary ammonium groups to the carboxylate groups, and thus amine naphthotubes **3a** and **3b** were synthesized. Consequently, the inward-pointing amine groups in **3a** and **3b** can be protonated and deprotonated by adjusting the pH value of the solution. The pK_a values of the two amine groups in **3b** were determined to be 8.7 and 9.9, respectively (Supplementary Figs. 1 and 2). At pH 7.4, both amine groups would be protonated. However, we found protonated **3a**•2H⁺ and **3b**•2H⁺ undergo serious aggregations in water (Supplementary Fig. 3). The critical aggregation concentration (CAC) for **3a**•2H⁺ is even below 0.05 mM, which prevents the study on its molecular recognition property. The aggregation should be caused by the recognition of carboxylate groups in the protonated cavity⁵⁸. Although protonated **3b**•2H⁺ has a higher CAC (0.16 mM, Supplementary Fig. 4) at pH 7.4, its binding property is very poor to the common organic guests (for most of the guests, K_a < 10³ M⁻¹, Supplementary Table 1 and Supplementary Figs. 5–21). Therefore, amine naphthotubes **3a** and **3b** are not appropriate to demonstrate stimuli-responsive molecular recognition. Consequently, new design is needed for realizing a pH-responsive *endo*-functionalized cavity.

Reducing the number of amine groups in amine naphthotubes **3** may be helpful to solve the aggregation problem. By combining the good binding ability of the amide naphthotubes **1** and the potential in pH-responsiveness of the amine naphthotubes **2**, one amide group and one secondary amine group are incorporated into the naphthotubes as the inward-directing functional groups (Fig. 2a). These naphthotubes with a pH-responsive *endo*-functionalized cavity possess low symmetry and are thus synthetically challenging when compared to the other naphthotubes²⁴. The hosts were synthesized by following a step-by-step procedure (see Supplementary Information): the secondary amine group was first constructed by intermolecular imine formation and then reduction; this is followed by intramolecular amide formation through the reaction between primary amine and carboxylate acid.

The *syn*- and *anti*-configurational isomers of the naphthotubes (**4a** and **4b**, Fig. 2b) with four ester sidechains were isolated in 8% and 11% yields, respectively, for the two steps. The two

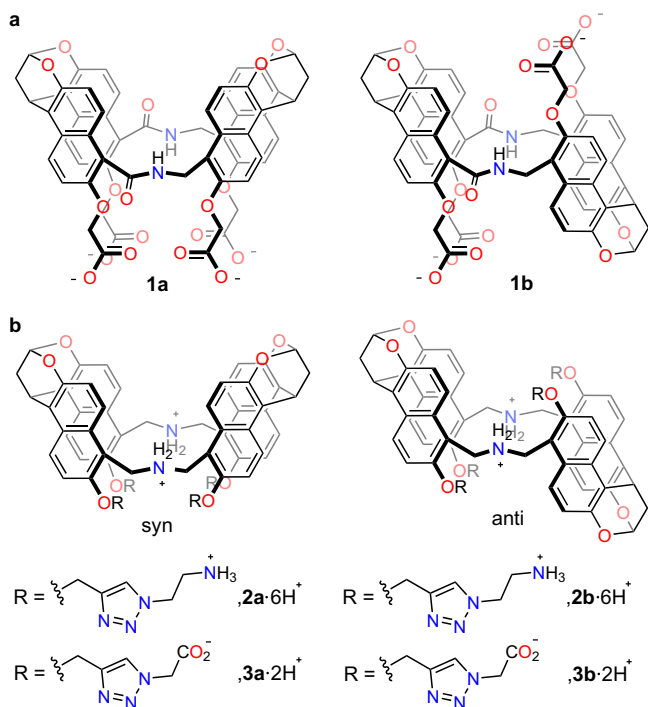


Fig. 1 Chemical structures of the amide and amine naphthotubes. **a** Amide naphthotubes (**1**). **b** Amine naphthotubes (**2** and **3**) with the secondary ammonium groups in the cavities.

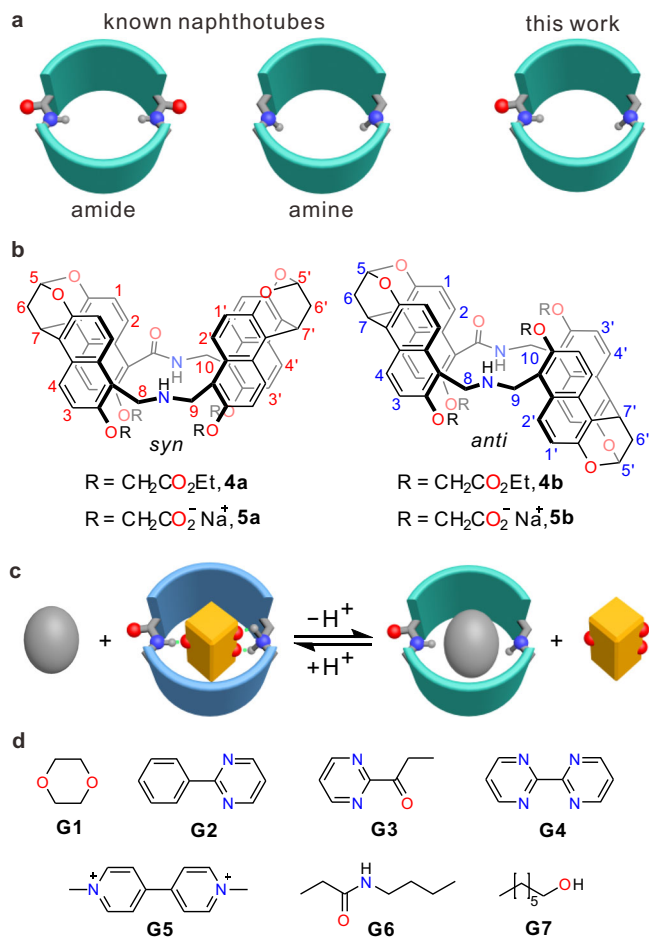


Fig. 2 Design concept of pH-responsive naphthotubes and chemical structures of the hosts and the guests involved in this research.

a Cartoon representation of the design of the pH-responsive naphthotubes by combining the features of amide and amine naphthotubes. The sidewalls of naphthotubes are colored as celeste; oxygen, red; nitrogen, blue.

b Chemical structures of the naphthotubes (**4** and **5**) with the amide and secondary amine groups in the cavities. **c** Cartoon representation of switchable bifunctional molecular recognition in water using the pH-responsive naphthotubes. The sidewalls of protonated naphthotubes are colored as blue. **d** Chemical structures of the guests involved in this research. The counter anion of **G5** is Cl⁻.

configurational isomers were assigned by 2D NMR spectra (Supplementary Figs. 22–25) and further confirmed by X-ray single crystallography. As shown in Fig. 3a, the secondary amine was protonated; the protons of the amide and ammonium groups were pointing toward the cavity and were thus shielded. The protonation of the amine group may be due to their high pK_a (dibenzylammonium, pK_a = 8.52 in water)⁶¹, and the counter anion PF₆⁻ should originate from the coupling agent PyBOP. After hydrolyzing the ester groups, water-soluble naphthotubes **5a** and **5b** were obtained. They have been further characterized in details by ¹H NMR, 2D NMR spectroscopy, and mass spectrometry (Supplementary Figs. 26–30).

The protonation and deprotonation states of **5a** and **5b** have been carefully studied in water (Fig. 3b). The pK_a values of **5a** and **5b** were determined to be 10.1 and 10.2, respectively, in water by ¹H NMR titrations (Fig. 3c and Supplementary Figs. 31 and 32) through fitting to the Henderson–Hasselbalch equation. The Hill coefficients for these experiments are close to 1.0 (for **5a**, 1.17; for **5b**, 1.24; Supplementary Table 2), supporting a two-state model.

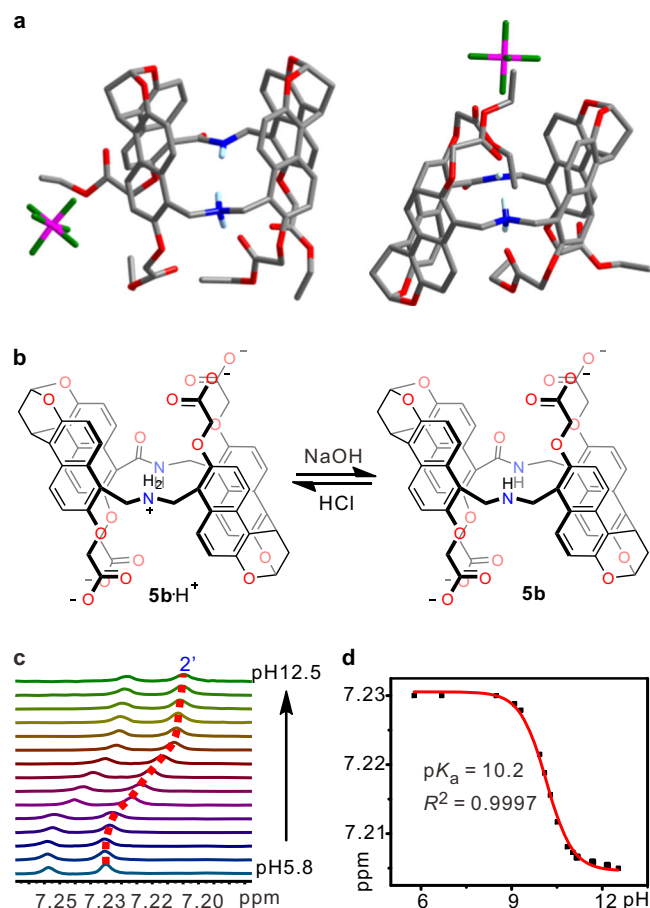


Fig. 3 X-ray single crystal structures of **4** and pK_a value determination of **5b**.

a X-ray single crystal structures of **4a** and **4b**. Solvent molecules and most of the hydrogen atoms are omitted for viewing clarity. Color codes: carbon, gray; oxygen, red; nitrogen, blue. **b** Interconversion between the protonated and deprotonated states of **5b**. **c** Partial ¹H NMR spectra of **5b** upon changing the pH values. **d** Titration curve tracking the change in the chemical shift of **5b** with changing the pH values, which was fit to the Henderson–Hasselbalch equation to determine pK_a value and Hill coefficient.

These values were further confirmed by fluorescence titrations (Supplementary Figs. 33 and 34). From the titration curves (Fig. 3d and Supplementary Figs. 31–34), it is clearly seen that the secondary amine group would be fully protonated at pH 7.4 and fully deprotonated at pH 12. Therefore, these two pH values were selected for the following guest-binding studies. These two states may show different binding behaviors (Fig. 2c). Moreover, the CAC of protonated **5a**•H⁺ and **5b**•H⁺ are more than 0.8 mM at pH 7.4 (Supplementary Fig. 35). All the titration experiments for the determination of association constants were performed at the host concentration lower than 0.5 mM to avoid the interference from aggregation.

Molecular recognition in water. The host–guest binding properties were studied in phosphate buffer at pH 7.4 and 12. At both the pH values, the carboxylate groups (pK_a = ~4.8)⁶¹ of the naphthotubes exist in the deprotonated state, thus providing water solubility for the hosts.

5a and **5b** have the similar cavity sizes as those of the amide naphthotubes. Therefore, typical guests for the amide naphthotubes, for example 1,4-dioxane (**G1**)⁵¹, aliphatic alcohols (**G7**)^{62,63} and phenyl pyrimidine (**G2**)⁵⁵ and their analogs (**G3**,

G4, and G6, Fig. 2d), were selected to study the binding behavior of 5a and 5b. In addition, methyl viologen (G5) was chosen as a guest as well because the cavities of these naphthotubes are electron-rich in the deprotonated state. These guests maintain in a neutral charge state at the used pH values because their pK_a values are smaller than 2 (Supplementary Table 3).

At pH 7.4, naphthotubes 5a and 5b were protonated and thus their cavities are positively charged. Therefore, they may not bind the positively charged guest G5 but may prefer to bind the guests with multiple hydrogen-bonding acceptors such as G2–G4. Indeed, when mixing the hosts and the guests in a 1:1 ratio at pD 7.4, ^1H NMR signals of both hosts and guests undergo significant changes (Supplementary Figs. 36–49) when compared to those of free guests and hosts. This is true for most of the guests but not for G5. This suggests that the protonated states of 5a•H⁺ and 5b•H⁺ are good hosts for the neutral guests. At pH 12, naphthotubes 5a and 5b exist in a non-protonated state. Their cavities are neutral and may prefer to bind hydrophobic guests and even positively charged guests such as G5. Except for G4, significant changes in the ^1H NMR spectra were observed (Supplementary Figs. 36–49) when mixing the hosts and the guests in solution at pD 12.

The binding affinities at the two pH values were further quantitatively studied. A 1:1 binding stoichiometry was assumed for all these host–guest pairs, which is supported by Job plots (Supplementary Figs. 50–53) and the knowledge on similar naphthotubes²⁴. The association constants of 5a and 5b to these typical guests were thus determined at pH 7.4 and 12 by ^1H NMR titrations (Supplementary Figs. 54–73) and the data are listed in Table 1.

In general, the *anti*-configurational isomer 5b is a better binder to these guests than the *syn*-configurational isomer 5a at both pH values. This is similar as the amide naphthotubes²⁴. As shown in Table 1, the binding affinities of 5a and 5b to the same guests are drastically different at pH 7.4 and 12. The association constants of G1–G4 are higher at pH 7.4 than those at pH 12. In contrast, G5–G7 have higher binding affinities at pH 12 than at pH 7.4. The ratios of the association constants at the two pH values for the same host–guest pair were also calculated and listed in Table 1. For the host–guest pairs of 5b with G4 and G5, the

association constants differ as large as 189 and 295 folds, respectively, at the two pH values. This clearly indicates that it is possible to drastically change the binding affinity of naphthotubes 5a and 5b to the same guests by simply adjusting the pH values and thus the protonation state of the host cavities. That is, the complexation of a guest by these hosts can be switched on and off by simply changing the pH value.

As mentioned above, naphthotubes 5a and 5b prefer to bind to guests G1–G4 with multiple hydrogen-bonding acceptors at pH 7.4. The association constants to G5–G7 are one to three orders of magnitude lower. In particular, no obvious binding was detected between 5b and G5. At pH 12, the association constants of naphthotubes 5a and 5b to these guests are at the range of 10 – 10^4 M⁻¹. G2 and G7 are preferred over other guests. However, the binding affinity of G2 is lower at pH 12 than at pH 7.4, and the binding affinity of G7 is higher at pH 12 than at pH 7.4. This interesting binding behavior would lay the basis for switching the complexed guests in the cavities of the naphthotubes through adjusting the pH values.

Binding mechanism. In order to reveal the thermodynamic binding behavior of these pH-responsive naphthotubes, the association constants and thermodynamic parameters of 5a and 5b to G1–G3 were determined by ITC titrations (Supplementary Figs. 74–87) at both pH 7.4 and 12. These three guests possess good water solubility and show large enough binding affinity for ITC titrations. The corresponding data are listed in Table 2.

The thermodynamic data may provide insights into the binding mechanism. As shown in Table 2, the bindings of all the six host–guest pairs are mainly enthalpy-driven with a favorable or unfavorable entropic contribution. For all the three guests, the association constants are higher at pH 7.4 than those at pH 12. The increased binding affinity at pH 7.4 is mainly originated from enthalpic gain. For guest G3, the entropic contribution are similar at both pH values for both the hosts, but their enthalpy differ significantly (for 5a, $\Delta\Delta H^\circ = -9$ kJ mol⁻¹; for 5b, $\Delta\Delta H^\circ = -9$ kJ mol⁻¹). This large difference in the enthalpy at two different pH values should originate from the different noncovalent interactions shielded in the hydrophobic cavity.

Similar as the amide naphthotubes^{51–54}, shielded hydrogen bonding and the hydrophobic effects through releasing the cavity waters^{64,65} or occupying the dry cavity⁶⁶ should be the main driving forces for the binding. Direct noncovalent interactions between hosts and guests can be analyzed using X-ray single crystal structures. However, single crystals of the host–guest complexes could not be obtained from water even after many trials. This may be attributed to the high water solubility of 5a and 5b. Fortunately, single crystal for the complex of 4b and G4 in CH₂Cl₂, suitable for X-ray crystallography, was obtained. The crystal structure was solved and shown in Fig. 4. Clearly, G4 is fully encapsulated in the cavity of 4b•H⁺. In addition, four hydrogen bonds were detected between the nitrogen atoms of the guest and the amide proton and the ammonium protons of the host. Noteworthy, the hydrogen bonds with the ammonium protons are charge-assisted. These hydrogen bonds should exist even in water because they are shielded in a hydrophobic microenvironment in the cavity⁶⁷. The binding mode and the binding driving force should be still valid in water where the hydrophobic effect also plays an important role. Nevertheless, desolvation of the protonated cavities of the naphthotubes is likely enthalpically more difficult, as indicated by the lower binding affinities to the hydrophobic guests (G5–G7) when compared to neutral naphthotubes. Therefore, this explains the reason why the naphthotubes prefer to bind the guests with multiple hydrogen-bonding acceptors at pH 7.4.

Table 1 Association constants (K_a , M⁻¹) of naphthotubes 5a and 5b with G1–G7 in phosphate buffer (50 mM, pH = 7.4 or 12, H₂O/D₂O = 9/1) at 298 K as determined by ^1H NMR titrations^a.

| Guest | Host | K_a (pH 7.4) | K_a (pH 12) | Ratio ^b |
|-------|------|-------------------------------|-------------------------------|--------------------|
| G1 | 5a | $(4.8 \pm 0.6) \times 10^3$ | $(1.6 \pm 0.2) \times 10^2$ | 30/1 |
| | 5b | $(3.8 \pm 0.7) \times 10^3$ | $(4.9 \pm 0.7) \times 10^2$ | 8/1 |
| G2 | 5a | $(8.4 \pm 0.1) \times 10^4$ c | $(2.4 \pm 0.4) \times 10^3$ c | 35/1 |
| | 5b | $(3.7 \pm 0.1) \times 10^5$ c | $(1.5 \pm 0.2) \times 10^4$ c | 25/1 |
| G3 | 5a | $(1.9 \pm 0.3) \times 10^4$ | $(6 \pm 1) \times 10^2$ | 32/1 |
| | 5b | $(1.1 \pm 0.1) \times 10^5$ | $(1.8 \pm 0.1) \times 10^3$ | 61/1 |
| G4 | 5a | $(8.6 \pm 0.2) \times 10^3$ c | $(5 \pm 1) \times 10^1$ | 172/1 |
| | 5b | $(1.7 \pm 0.2) \times 10^4$ c | $(9 \pm 2) \times 10^1$ | 189/1 |
| G5 | 5a | - ^d | - ^d | - ^d |
| | 5b | $(2.0 \pm 0.4) \times 10^1$ | $(5.9 \pm 0.9) \times 10^3$ | 1/295 |
| G6 | 5a | $(7 \pm 1) \times 10^1$ | $(7.0 \pm 0.6) \times 10^2$ | 1/10 |
| | 5b | $(1.0 \pm 0.1) \times 10^2$ | $(1.6 \pm 0.1) \times 10^3$ | 1/16 |
| G7 | 5a | $(1.0 \pm 0.1) \times 10^3$ | $(5.6 \pm 0.7) \times 10^3$ | 1/6 |
| | 5b | $(2.0 \pm 0.4) \times 10^3$ | $(4.0 \pm 0.4) \times 10^4$ | 1/20 |

^aThe data were averaged from three independent titrations.

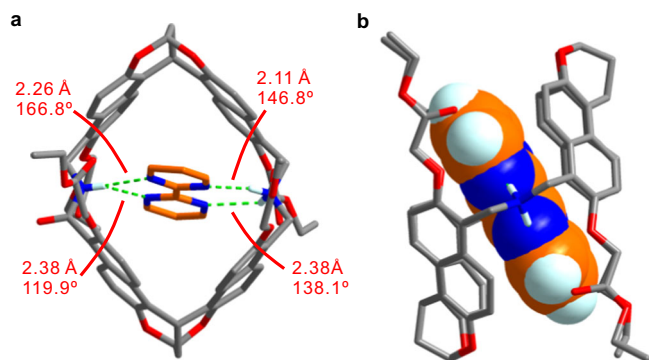
^bRatio = K_a (pH 7.4)/ K_a (pH 12).

^cThese association constants were determined by ITC titrations.

^dThe association constants could not be obtained due to severe aggregation in the host–guest mixture.

Table 2 Association constants (K_a , M^{-1}) and thermodynamic parameters (ΔH° and $-T\Delta S^\circ$, kJ mol^{-1}) of naphthotubes **5a and **5b** with **G1**–**G3** in phosphate buffer (50 mM, pH = 7.4 or 12, H_2O) at 298 K as determined by ITC titrations^a.**

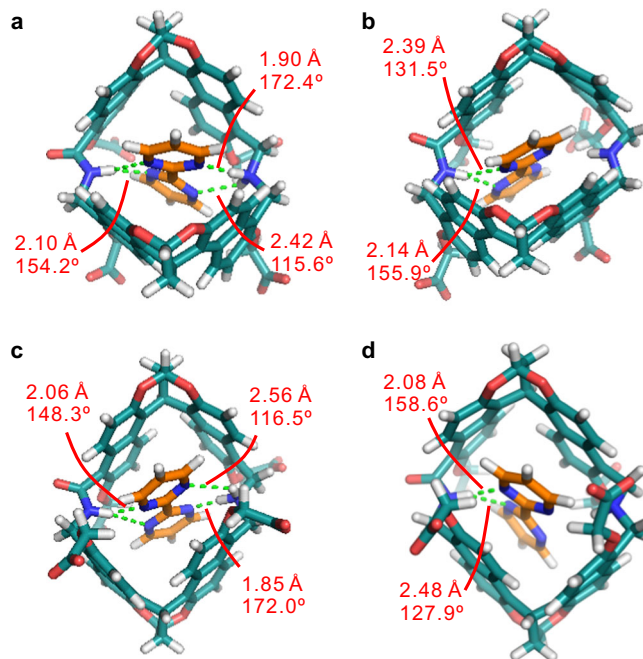
| Guest | Host | pH 7.4 | | | pH 12 | | |
|-----------|-----------|-----------------------------|------------------|--------------------|-----------------------------|------------------|--------------------|
| | | K_a | ΔH° | $-T\Delta S^\circ$ | K_a | ΔH° | $-T\Delta S^\circ$ |
| G1 | 5a | $(4.5 \pm 0.2) \times 10^3$ | -35 ± 4 | 14 ± 4 | $(2.5 \pm 0.2) \times 10^2$ | -10.3 ± 0.1 | -3.3 ± 0.2 |
| | 5b | $(4.4 \pm 0.1) \times 10^3$ | -18 ± 1 | -2 ± 1 | $(5.0 \pm 0.3) \times 10^2$ | -15 ± 2 | -1 ± 2 |
| G2 | 5a | $(8.4 \pm 0.1) \times 10^4$ | -42.4 ± 0.5 | 14.3 ± 0.5 | $(2.4 \pm 0.4) \times 10^3$ | -22 ± 2 | 2 ± 2 |
| | 5b | $(3.7 \pm 0.1) \times 10^5$ | -36 ± 1 | 4.2 ± 0.9 | $(1.5 \pm 0.2) \times 10^4$ | -30 ± 3 | 7 ± 3 |
| G3 | 5a | $(2.0 \pm 0.2) \times 10^4$ | -29 ± 2 | 5 ± 2 | $(5.8 \pm 0.3) \times 10^2$ | -20 ± 2 | 5 ± 2 |
| | 5b | $(9.4 \pm 0.3) \times 10^4$ | -28 ± 2 | -1 ± 2 | $(1.7 \pm 0.1) \times 10^3$ | -19 ± 1 | 1 ± 1 |

^aThe data were averaged from three independent titrations.**Fig. 4 X-ray single crystal structure of $\text{G4@4b} \cdot \text{H}^+$.** **a** The over view of $\text{G4@4b} \cdot \text{H}^+$ is presented as a stick model, showing four hydrogen bonds between guest and host. **b** Host and guest are shown with stick model and space-filling model in the side view of $\text{G4@4b} \cdot \text{H}^+$, respectively. **G4** is fully encapsulated in the cavity of $\text{4b} \cdot \text{H}^+$. Most of hydrogen atoms and PF_6^- counter ions are omitted for viewing clarity. Color codes: carbon, gray or orange; oxygen, red; nitrogen, blue.

To further reveal the binding mechanism in water at both pH values, DFT calculations on the complexes of **G4** with **5a** and **5b** in water were performed with the host to be protonated and deprotonated. As shown in Fig. 5, the binding mode and the geometry for the complex of **5b** and **G4** are similar to those of the crystal structure of the complex of **4b** and **G4** at the protonated state. This supports our reasoning that the binding mode in an *endo*-functionalized cavity should not be significantly affected by solvents. Similar binding mode was observed for the complex of **G4** and **5a**. At the deprotonated state, the guest only forms hydrogen bonds with the amide protons of the hosts. Thus, the binding affinity is significantly weakened at pH 12.

From the above analysis, protonation and deprotonation of the secondary amine of the naphthotubes drastically change the cavity feature and thus the direct noncovalent interactions between the hosts and the guests. This would then change the binding preferences of the hosts at the two pH values. For the complexes between **G5** and nonprotonated naphthotubes **5**, the binding is mainly driven by the hydrophobic effect and cation- π interactions. Nevertheless, tetramethylammonium shows very weak binding to **5** (Supplementary Fig. 88), which may be due to unmatched shape and size. In addition, the weak binding between **G5** and protonated naphthotubes **5** should result from the charge repulsion between the charged cavity and charged guests.

Switchable Bifunctional molecular recognition. To achieve switchable bifunctional molecular recognition, it needs two guests which are the best binders to the naphthotubes at the protonation

**Fig. 5 Binding modes between **5** and **G4**.** Energy-minimized structures of (a) $\text{G4@5a} \cdot \text{H}^+$, (b) G4@5a , (c) $\text{G4@5b} \cdot \text{H}^+$ and (d) G4@5b calculated by DFT calculations (wB97XD/6-311 + G(d) and 6-311 G(d)) with the PCM solution model in water at 298 K. Color codes: carbon, celeste or orange; oxygen, red; nitrogen, blue.

and deprotonation states, respectively. In addition, the two guests should also have drastically different binding affinities at the two states of the hosts to enable clear-cut differentiation. Naphthotube **5b** is usually a better binder to these guests than **5a**. Therefore, **5b** is selected as the host for the demonstration. Guests **G4** and **G5** have the largest differences in the association constants at the two states of **5b** and are thus selected as the guests.

First, the switchable binding was demonstrated in a binary system with **5b** and **G4/G5**. **5b** shows very high binding affinity to **G4** at pH 7.4 ($K_a = 1.7 \times 10^4 M^{-1}$), but binds very weakly to **G4** at pH 12 ($K_a = 90 M^{-1}$). In contrast, **5b** binds **G5** strongly ($K_a = 5.9 \times 10^3 M^{-1}$) at pH 12 and weakly ($K_a = 20 M^{-1}$) at pH 7.4. The large differences in the binding affinities at the two states would allow an on-off/off-on switch in the binary mixtures. Indeed, when increasing the pH values of the solution containing **5b** and **G4** at pH 7.4 through gradually adding 8 equivalents of NaOH, the proton signals of **G4** shift downfield to the position of free **G4** (Supplementary Fig. 89). The ^1H NMR spectra is the superposition of free **G4** and free but deprotonated **5b** at pH 12. This suggests that **G4** is released from the cavity of **5b** when the

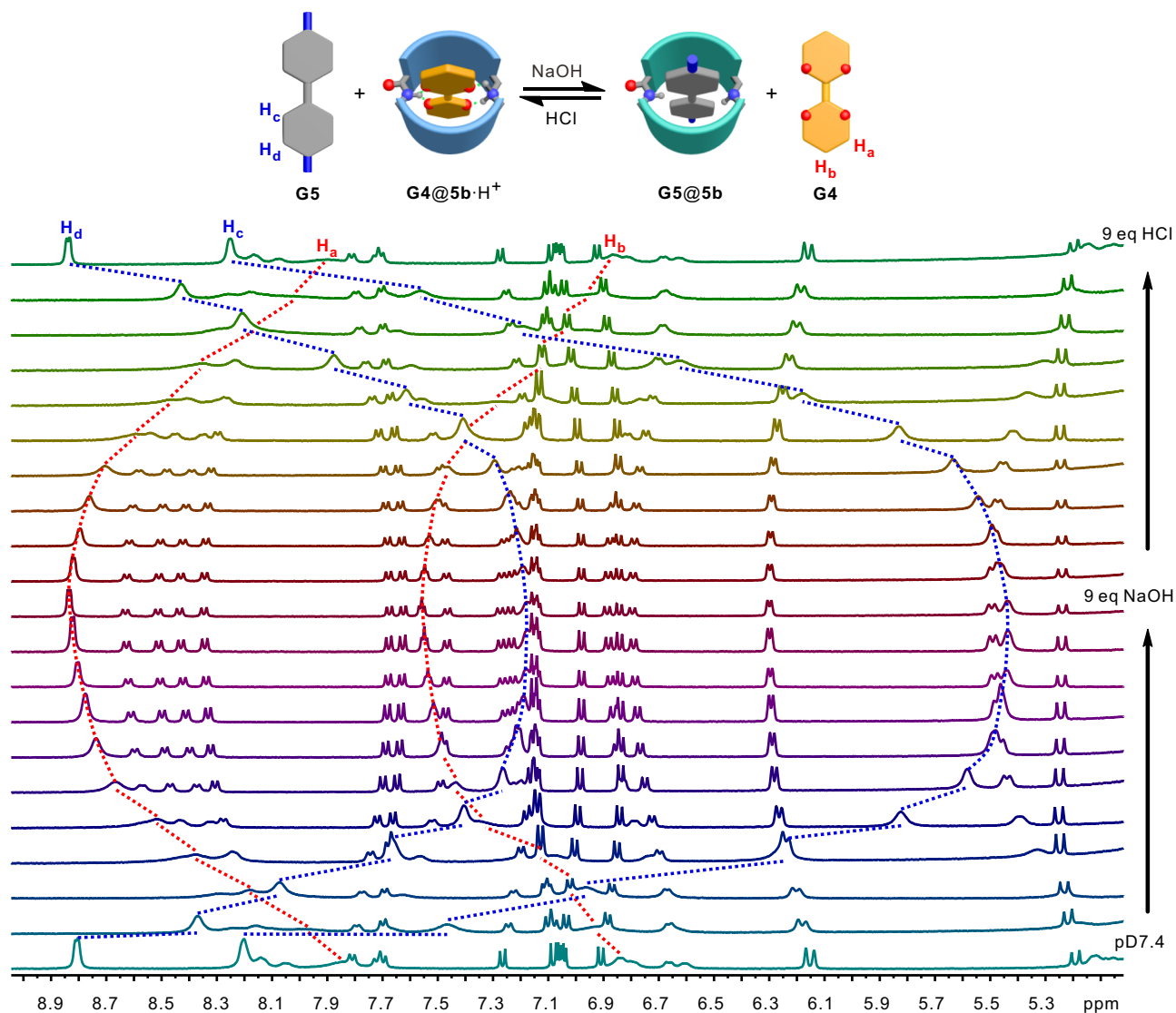


Fig. 6 Switchable bifunctional molecular recognition. Cartoon representation of switchable bifunctional molecular recognition and partial ^1H NMR spectra (500 MHz, D_2O) of the equimolar mixture of **5b**, **G4** and **G5** at pD 7.4 after gradually adding 9 equivalents of NaOH and then 9 equivalents of HCl.

cavity is deprotonated after adding NaOH. The ^1H NMR spectra can be restored after adding 8 equivalents of HCl. This indicates that **G4** can be up-taken again into the cavity of **5b** after protonation. The two processes are reversible. Similar phenomena are observed for the binary mixture of **5b** and **G5** (Supplementary Fig. 90). Differently, **G5** was taken up into the cavity of **5b** at the deprotonation state and kicked out from the cavity at the protonation state.

Finally, switchable bifunctional molecular recognition was demonstrated with the ternary mixture of **5b**, **G4** and **G5**. The solution was prepared in D_2O and the initial pD is determined to be ca. 7.4. The ^1H NMR spectra (Fig. 6) is the superposition of the spectra of free **G5** and the complex of **5b**· H^+ and **G4** (Supplementary Fig. 91). After gradually adding 9 equivalents of NaOH, the ^1H NMR spectra undergo large changes, and the spectrum is the superposition of the spectra of free **G4** and the complex of **5b** and **G5**. This suggests guest **G4** in the cavity of **5b**· H^+ is kicked out and swapped with **G5** after converting **5b**· H^+ to **5b** through deprotonation. This shows **5b** is able to perform switchable bifunctional molecular recognition in the ternary mixture of **5b**, **G4** and **G5**. Moreover, the system can be restored to its original state through adding 9 equivalents of HCl to the

above solution (Fig. 6), showing the good reversibility of the system.

In summary, we reported a pair of biomimetic macrocyclic hosts with a pH-responsive *endo*-functionalized cavity. These naphthotubes possess two inward-directing functional groups, amide and secondary amine, in their cavities. The secondary amine group can be protonated at pH 7.4 and deprotonated at pH 12. Thus, the cavity features of the naphthotubes can be switched between the two states. Therefore, the naphthotubes show drastically different guest-binding preferences at the two pH values. Further research reveals that the noncovalent interactions between the hosts and the guests are different at the two host states, leading to different binding preference and selectivity. The guest-binding behavior of the naphthotubes can be simply tuned by adjusting the pH value in the solution. In a ternary mixture of one host with two guests, the guest molecules can be selectively up-taken into the cavity of the host by changing the pH value and thus the cavity states. These biomimetic macrocyclic hosts with selective and switchable recognition properties at different pH values are interesting for water-soluble synthetic hosts. The binding affinity may be too small for noncovalent bioconjugation²⁵, but these hosts may still find applications in

the fields of self-assembly, water-soluble molecular machines, environmental sciences and biomedical sciences.

Methods

General. All the reagents and guest molecules involved in this research were commercially available and used without further purification unless otherwise noted. ^1H , ^{13}C NMR, ^1H - ^1H COSY and ^1H - ^1H ROESY NMR spectra were recorded on Bruker Avance-400 (500) spectrometers. Electrospray-ionization time-of-flight high-resolution mass spectrometry (ESI-TOF-HRMS) experiments were conducted on an applied Q EXACTIVE mass spectrometry system. Fluorescence spectra were obtained on a Shimadzu RF-5301pc spectrometer.

Synthesis and characterization. Synthesis and the corresponding characterization data are provided in the Supplementary Information.

Determination of the association constants. To determine the association constants, NMR titrations and ITC titrations were performed in phosphate buffer (50 mM, pH = 7.4 or 12) at 298 K. NMR titrations were carried out by adding guest to the solution of host with a fixed concentration. Non-linear curve-fitting was then performed on the plots of δ_{obs} of host as a function of $[G]$ to obtain the association constants (K_a). In a typical ITC titration experiment, a 1.4338 mL solution of host was placed in the sample cell, and 292 μL of a solution of guest was in the injection syringe. Heats of dilution, measured by titration of guest into the sample cell with blank solvent, were subtracted from each data set. All solutions were degassed prior to titration. The data were analyzed using the instrumental internal software package and fitted by “one set of binding sites” model to give the association constants (K_a). Non-linear fitting data are shown in Supplementary Figs. 12–21, 54–73 and 88. ITC titration data are shown in Supplementary Figs. 74–87.

Data availability

The X-ray crystallographic coordinates for structures reported in this study have been deposited at the Cambridge Crystallographic Data Centre (CCDC), under deposition numbers 2106751 (4a), 2106752 (4b) and 2106753 (G4@4b). These data can be obtained free of charge from the Cambridge Crystallographic Data Centre via www.ccdc.cam.ac.uk/data_request/cif. All other data supporting the findings of this study are available within the Article and its Supplementary Information and/or from the corresponding author upon request.

Received: 23 December 2021; Accepted: 8 April 2022;

Published online: 28 April 2022

References

- Chatterji, D. *Basics of Molecular Recognition* (CRC Press, Boca Raton, 2016).
- Crini, G. Review: a history of cyclodextrins. *Chem. Rev.* **114**, 10940–10975 (2014).
- Barrow, S. J., Kasera, S., Rowland, M. J., del Barrio, J. & Scherman, O. A. Cucurbituril-based molecular recognition. *Chem. Rev.* **115**, 12320–12406 (2015).
- Murray, J., Kim, K., Ogoshi, T., Yao, W. & Gibb, B. C. The aqueous supramolecular chemistry of cucurbit[n]urils, pillar[n]arenes and deep-cavity cavitands. *Chem. Soc. Rev.* **46**, 2479–2496 (2017).
- Liu, W., Samanta, S. K., Smith, B. D. & Isaacs, L. Synthetic mimics of biotin/(strept)avidin. *Chem. Soc. Rev.* **46**, 2391–2403 (2017).
- Yu, Y. & Rebek, J. Jr. Reactions of folded molecules in water. *Acc. Chem. Res.* **51**, 3031–3040 (2018).
- Oshovsky, G. V., Reinhoudt, D. N. & Verboom, W. Supramolecular chemistry in water. *Angew. Chem. Int. Ed.* **46**, 2366–2393 (2007).
- Kataev, E. A. & Mueller, C. Recent advances in molecular recognition in water: artificial receptors and supramolecular catalysis. *Tetrahedron* **70**, 137–167 (2014).
- Persch, E., Dumele, O. & Diederich, F. Molecular recognition in chemical and biological systems. *Angew. Chem. Int. Ed.* **54**, 3290–3327 (2015).
- Kubik, S. *Supramolecular Chemistry in Water* (Wiley-VCH, Weinheim, 2019).
- Cremer, P. S., Flood, A. H., Gibb, B. C. & Mobley, D. L. Collaborative routes to clarifying the murky waters of aqueous supramolecular chemistry. *Nat. Chem.* **10**, 8–16 (2018).
- Escobar, L. & Ballester, P. Molecular recognition in water using macrocyclic synthetic receptors. *Chem. Rev.* **121**, 2445–2514 (2021).
- Dong, J. & Davis, A. P. Molecular recognition mediated by hydrogen bonding in aqueous media. *Angew. Chem. Int. Ed.* **60**, 8035–8048 (2021).
- Davis, A. P., Kubik, S. & Dalla Cort, A. Editorial: supramolecular chemistry in water. *Org. Biomol. Chem.* **13**, 2499–2500 (2015).
- Anslyn, E. V. & Dougherty, D. A. *Modern Physical Organic Chemistry*, 230–232 (University Science Books, Sausalito, 2006).
- Davis, A. P. Biomimetic carbohydrate recognition. *Chem. Soc. Rev.* **49**, 2531–2545 (2020).
- Butterfield, S. M. & Rebek, J. Jr. A synthetic mimic of protein inner space: buried polar interactions in a deep water-soluble host. *J. Am. Chem. Soc.* **128**, 15366–15367 (2006).
- Verdejo, B., Gil-Ramirez, G. & Ballester, P. Molecular recognition of pyridine N-oxides in water using calix[4]pyrrole receptors. *J. Am. Chem. Soc.* **131**, 3178–3179 (2009).
- Escobar, L., Diaz-Moscoso, A. & Ballester, P. Conformational selectivity and high-affinity binding in the complexation of N-phenyl amides in water by a phenyl extended calix[4]pyrrole. *Chem. Sci.* **9**, 7186–7192 (2018).
- Peñuelas-Haro, G. & Ballester, P. Efficient hydrogen bonding recognition in water using aryl-extended calix[4]pyrrole receptors. *Chem. Sci.* **10**, 2413–2423 (2019).
- Chi, X., Zhang, H., Vargas-Zúñiga, G. I., Peters, G. M. & Sessler, J. L. A dual-responsive bola-type supra-amphiphile constructed from a water-soluble calix[4]pyrrole and a tetraphenylthene-containing pyridine bis-N-oxide. *J. Am. Chem. Soc.* **138**, 5829–5832 (2016).
- Peck, E. M. et al. Rapid macrocycle threading by a fluorescent dye-polymer conjugate in water with nanomolar affinity. *J. Am. Chem. Soc.* **137**, 8668–8671 (2015).
- Liu, W., Johnson, A. & Smith, B. D. Guest back-folding: a molecular design strategy that produces a deep-red fluorescent host/guest pair with picomolar affinity in water. *J. Am. Chem. Soc.* **140**, 3361–3370 (2018).
- Yang, L.-P., Wang, X., Yao, H. & Jiang, W. Naphthotubes: macrocyclic hosts with a biomimetic cavity feature. *Acc. Chem. Res.* **53**, 198–208 (2020).
- Ma, Y.-L. et al. Biomimetic recognition-based bioorthogonal host-guest pairs for cell targeting and tissue imaging in living animals. *CCS Chem.* **3**, 2143–2155 (2021).
- Wang, L.-L. et al. Molecular recognition and chirality sensing of epoxides in water using endo-functionalized molecular tubes. *J. Am. Chem. Soc.* **139**, 8436–8439 (2017).
- Wang, L.-L., Quan, M., Yang, T.-L., Chen, Z. & Jiang, W. A green and wide-scope approach for chiroptical sensing of organic molecules through biomimetic recognition in water. *Angew. Chem. Int. Ed.* **59**, 23817–23824 (2020).
- Yang, L.-P., Ke, H., Yao, H. & Jiang, W. Effective and rapid removal of polar organic micropollutants from water by amide naphthotube-crosslinked polymers. *Angew. Chem. Int. Ed.* **60**, 21404–21411 (2021).
- Tromans, R. A. et al. A biomimetic receptor for glucose. *Nat. Chem.* **11**, 52–56 (2019).
- Tromans, R. A., Samanta, S. K., Chapman, A. M. & Davis, A. P. Selective glucose sensing in complex media using a biomimetic receptor. *Chem. Sci.* **11**, 3223–3227 (2020).
- Zhang, M., Yan, X., Huang, F., Niu, Z. & Gibson, H. W. Stimuli-responsive host-guest systems based on the recognition of cryptands by organic guests. *Acc. Chem. Res.* **47**, 1995–2005 (2014).
- Xue, M., Yang, Y., Chi, X., Yan, X. & Huang, F. Development of pseudorotaxanes and rotaxanes: from synthesis to stimuli-responsive motions to applications. *Chem. Rev.* **115**, 7398–7501 (2015).
- Qu, D.-H., Wang, Q.-C., Zhang, Q.-W., Ma, X. & Tian, H. Photoresponsive host-guest functional systems. *Chem. Rev.* **115**, 7543–7588 (2015).
- Knipe, P. C., Thompson, S. & Hamilton, A. D. Ion-mediated conformational switches. *Chem. Sci.* **6**, 1630–1639 (2015).
- Blanco-Gomez, A. et al. Controlled binding of organic guests by stimuli-responsive macrocycles. *Chem. Soc. Rev.* **49**, 3834–3862 (2020).
- Jie, K., Zhou, Y., Yao, Y., Shi, B. & Huang, F. CO₂-responsive pillar[5]arene-based molecular recognition in water: establishment and application in gas-controlled self-assembly and release. *J. Am. Chem. Soc.* **137**, 10472–10475 (2015).
- Catti, L., Kishida, N., Kai, T., Akita, M. & Yoshizawa, M. Polyaromatic nanocapsules as photoresponsive hosts in water. *Nat. Commun.* **10**, 1948 (2019).
- Duan, Q., Zhang, H., Mai, W., Wang, F. & Lu, K. Acid/base- and base/acid-switchable complexation between anionic-/cationic-pillar[6]arenes and a viologen ditosylate salt. *Org. Biomol. Chem.* **17**, 4430–4434 (2019).
- Schreiber, C. L. & Smith, B. D. Molecular conjugation using non-covalent click chemistry. *Nat. Rev. Chem.* **3**, 393–400 (2019).
- Zhang, T.-X. et al. A general hypoxia-responsive molecular container for tumor-targeted therapy. *Adv. Mater.* **32**, 1908435 (2020).
- Kay, E. R., Leigh, D. A. & Zerbetto, F. Synthetic molecular motors and mechanical machines. *Angew. Chem. Int. Ed.* **46**, 72–191 (2007).
- Coskun, A., Banaszak, M., Astumian, R. D., Stoddart, J. F. & Grzybowski, B. A. Great expectations: can artificial molecular machines deliver on their promise? *Chem. Soc. Rev.* **41**, 19–30 (2012).

43. Erbas-Cakmak, S., Leigh, D. A., McTernan, C. T. & Nussbaumer, A. L. Artificial molecular machines. *Chem. Rev.* **115**, 10081–10206 (2015).
44. Stoddart, J. F. Mechanically interlocked molecules (MIMs)—molecular shuttles, switches, and machines (Nobel Lecture). *Angew. Chem. Int. Ed.* **56**, 11094–11125 (2017).
45. Baroncini, M., Silvi, S. & Credi, A. Photo- and redox-driven artificial molecular motors. *Chem. Rev.* **120**, 200–268 (2020).
46. Dattler, D. et al. Design of collective motions from synthetic molecular switches, rotors, and motors. *Chem. Rev.* **120**, 310–433 (2020).
47. Ji, X. et al. Removal of organic micropollutants from water by macrocycle-containing covalent polymer networks. *Angew. Chem. Int. Ed.* **59**, 23402–23412 (2020).
48. Klemes, M. J. et al. Polymerized molecular receptors as adsorbents to remove micropollutants from water. *Acc. Chem. Res.* **53**, 2314–2324 (2020).
49. Skorjanc, T., Shetty, D. & Trabolzi, A. Pollutant removal with organic macrocycle-based covalent organic polymers and frameworks. *Chem* **7**, 882–918 (2021).
50. Zhou, H. et al. Biomimetic recognition of quinones in water by an endo-functionalized cavity with anthracene sidewalls. *Angew. Chem. Int. Ed.* **60**, 25981–25987 (2021).
51. Huang, G.-B., Wang, S.-H., Ke, H., Yang, L.-P. & Jiang, W. Selective recognition of highly hydrophilic molecules in water by endo-functionalized molecular tubes. *J. Am. Chem. Soc.* **138**, 14550–14553 (2016).
52. Yao, H. et al. Molecular recognition of hydrophilic molecules in water by combining the hydrophobic effect with hydrogen bonding. *J. Am. Chem. Soc.* **140**, 13466–13477 (2018).
53. Ke, H. et al. Shear-induced assembly of a transient yet highly stretchable hydrogel based on pseudopolyrotaxanes. *Nat. Chem.* **11**, 470–477 (2019).
54. Li, S., Yao, H., Kameda, T., Jiang, W. & Kitahara, R. Volumetric properties for the binding of 1,4-dioxane to amide naphthotubes in water. *J. Phys. Chem. B* **124**, 9175–9181 (2020).
55. Ma, Y.-L. et al. Biomimetic recognition of organic drug molecules in water by amide naphthotubes. *CCS Chem.* **2**, 1078–1092 (2021).
56. Liu, W.-E. et al. Stabilization of the closed-ring isomer of spiropyran by amide naphthotube in water and its application in naked-eye detection of toxic paraoxon. *ChemPhysChem* **21**, 2249–2253 (2020).
57. Chai, H. et al. Enantioselective recognition of neutral molecules in water by a pair of chiral biomimetic macrocyclic receptors. *CCS Chem.* **2**, 440–452 (2020).
58. Huang, X. et al. Biomimetic recognition and optical sensing of carboxylic acids in water by using a buried salt bridge and the hydrophobic effect. *Angew. Chem. Int. Ed.* **60**, 1929–1935 (2021).
59. Cui, J.-S. et al. Directional shuttling of a stimuli-responsive cone-like macrocycle on a single-state symmetric dumbbell axle. *Angew. Chem. Int. Ed.* **57**, 7809–7814 (2018).
60. Zheng, L.-S., Cui, J.-S. & Jiang, W. Biomimetic synchronized motion of two interacting macrocycles in [3]Rotaxane-based molecular shuttles. *Angew. Chem. Int. Ed.* **58**, 15136–15141 (2019).
61. <http://ibond.nankai.edu.cn/pka/> Date of access: November 20, 2021.
62. Shorthill, B. J., Avetta, C. T. & Glass, T. E. Shape-selective sensing of lipids in aqueous solution by a designed fluorescent molecular tube. *J. Am. Chem. Soc.* **126**, 12732–12733 (2004).
63. Avetta, C. T., Shorthill, B. J., Ren, C. & Glass, T. E. Molecular tubes for lipid sensing: tube conformations control analyte selectivity and fluorescent response. *J. Org. Chem.* **77**, 851–857 (2012).
64. Biedermann, F., Nau, W. M. & Schneider, H.-J. The hydrophobic effect revisited—studies with supramolecular complexes imply high-energy water as a noncovalent driving force. *Angew. Chem. Int. Ed.* **53**, 11158–11171 (2014).
65. Snyder, P. W., Lockett, M. R., Moustakas, D. T. & Whitesides, G. M. Is it the shape of the cavity, or the shape of the water in the cavity? *Eur. Phys. J. Spec. Top.* **223**, 853–891 (2014).
66. Barnett, J. W. et al. Spontaneous drying of non-polar deep-cavity cavitand pockets in aqueous solution. *Nat. Chem.* **12**, 589–594 (2020).
67. Gao, J., Bosco, D. A., Powers, E. T. & Kelly, J. W. Localized thermodynamic coupling between hydrogen bonding and microenvironment polarity substantially stabilizes proteins. *Nat. Struct. Mol. Biol.* **16**, 684–690 (2009).

Acknowledgements

This research was financially supported by the National Natural Science Foundation of China (No. 22125105, W.J.), the Shenzhen Science and Technology Innovation Committee (JCYJ20180504165810828, W.J.), Shenzhen “Pengcheng Scholar”, Guangdong Provincial Key Laboratory of Catalysis (No. 2020B121201002, W.J.), and Guangdong High-Level Personnel of Special Support Program (2019TX05C157, W.J.). We are grateful to Dr. Xiaoyong Chang for the help on X-ray crystallography, the technical support from SUSTech-CRF and the Center for Computational Science and Engineering of SUSTech.

Author contributions

W.J. conceived and designed the experiments. X.W. carried out the experimental work. M.Q. performed the DFT calculations. H.Y., X.-Y.P. and H.K. solved the crystal structure. W.J. and X.W. analyzed the data and wrote the manuscript, and all the authors commented on it.

Competing interests

The authors declare no competing interests.

Additional information


Supplementary information The online version contains supplementary material available at <https://doi.org/10.1038/s41467-022-30012-4>.

Correspondence and requests for materials should be addressed to Wei Jiang.

Peer review information *Nature Communications* thanks Pau Ballester and the other, anonymous, reviewer(s) for their contribution to the peer review of this work. Peer reviewer reports are available.

Reprints and permission information is available at <http://www.nature.com/reprints>

Publisher's note Springer Nature remains neutral with regard to jurisdictional claims in published maps and institutional affiliations.

 **Open Access** This article is licensed under a Creative Commons Attribution 4.0 International License, which permits use, sharing, adaptation, distribution and reproduction in any medium or format, as long as you give appropriate credit to the original author(s) and the source, provide a link to the Creative Commons license, and indicate if changes were made. The images or other third party material in this article are included in the article's Creative Commons license, unless indicated otherwise in a credit line to the material. If material is not included in the article's Creative Commons license and your intended use is not permitted by statutory regulation or exceeds the permitted use, you will need to obtain permission directly from the copyright holder. To view a copy of this license, visit <http://creativecommons.org/licenses/by/4.0/>.

© The Author(s) 2022